ON THE OPTIMIZATION OF A CENTRAL RECEIVER SYSTEM

Jaap E Hoffmann[1]

[1] Department of Mechanical and Mechatronic Engineering

Stellenbosch University, Stellenbosch, South Africa; Phone: +27 – 21 – 808 - 3554; E-Mail: hoffmaj@sun.ac.za

Abstract

The optical field and receiver system contributes up to 50 % to the total cost of a central receiver solar power plant. Most optimization studies focus on a given heliostat design and seek to optimize the field layout for maximum collection efficiency. Heliostat size seems to be a controversial topic with research leading to conflicting results. Formal mathematic optimization, solving a set of sequential spherical quadratic sub-problems, was used to optimize the collection efficiency of a central receiver system with a biomimetic heliostat field arrangement, subject to a non-interference constraint. The design variables are receiver optical height, receiver height and diameter, heliostat length and width, and the seeding parameters for radial and azimuthal spacing of the optical field. An optimum annual averaged field efficiency of 64.0 % was calculated, up from the initial field efficiency of 57.7 %. The optimal heliostat size is 184 m^2, and receiver width follows the growth in heliostat size closely. The collection efficiency is relatively insensitive to tower optical height. It is clear from literature that different objective functions will drive results towards conflicting outputs. The choice of objective function will most likely be driven by the researcher's role within the concentrating solar power community.

Keywords: central receiver, heliostat field, biomimetic layout, collection efficiency, mathematical optimization.

1. Introduction

The heliostat field is the dominant capital cost of a central receiver plant, contributing 40 – 50 % of the total plant cost, depending on the amount of thermal energy storage [1, 2]. Despite the use of free energy from the sun, solar thermal energy is still considerably more expensive than fossil fuel derived power, and other forms of renewable energy, like wind, hydro, and photovoltaics. With thermal energy storage, solar thermal energy is an attractive solution for future power generation in an arid country like South Africa with a high solar resource, but limited wind and hydro resources. Efforts to reduce the cost of the heliostat field is mainly focussed on either reducing the cost of individual heliostats [3, 4], or reducing the total number of heliostats via an improved field lay-out. These, and other plant improvements supports the SunShot Initiative's long term goal of solar thermal energy being cost competitive with fossil fuel derived power generation.

One of the earliest studies in heliostat field optimization was done by Lipps and Van't Hull [3], who concluded that the overall collection efficiency of staggered heliostat fields is usually higher than that of a cornfield lay-out. They used the ratio between total system cost to the total energy collected as figure of merit. In order to reduce the number of calculations, individual heliostats were replaced by cells of representative heliostats. Sanchez and Romero [6] suggested the use of a growth based algorithm to design the heliostat field lay-out. The first heliostat is placed in the position that yields the highest yearly energy collection, the second heliostat is placed in the next best position, considering blocking and shading by the first, and so forth until the entire field is populated. Wei et al [7] focused on the heliostat field for a cavity receiver, and concluded that there is a relationship between the effective field boundaries and cavity aperture geometry. Ausburger [8] used a multi-variable optimization routine to find the lowest levelized cost of electricity (LCOE) for the radially staggered Gemasolar heliostat field. Heliostat spacing, size, number of heliostats, receiver optical height, and receiver length and diameter were all treated as design variables. He concluded that the plant with the lowest LCOE also has the lowest optical efficiency, mainly due to the increased attenuation and spillage losses associated with larger fields. Besarati and Goswami [9] optimized a biomimetic heliostat field lay-out for a 50 MW_t plant at Dagget, California, using maximum field efficiency as target function for a fixed tower height and heliostat size. They validated their model against field measurements at the PS10 plant in Andalucia, Spain, and subsequently used it to redesign the PS10 heliostat field lay-out. Carizosa at al [10] used a greedy-based algorithm to optimize the electricity generated per unit cost for a heliostat field comprised off different sized heliostats in the same field. Lutchman et al [11] assigned a random location to each heliostat in a bounded field, and used a

constrained classical gradient based optimization algorithm to force heliostats towards positions that maximize the field optical efficiency. The heliostat position vector for each heliostat is treated as a design variable. Pidaparthi and Hoffmann [12] investigated the effect of three discrete heliostat sizes on the LCOE for a 100 MW_e solar thermal power plant at Upington, South Africa, and concluded that medium sized heliostats (43 m^2) yield the lowest LCOE. The research cited in the introduction is not meant to be comprehensive, but rather highlight distinctive trends followed by individual researchers/research groups.

Numerous software tools (HFLCAL, DELSOL3, CAMPO, SOLTRACE, SAM, SolarPILOT, etc.) have been developed to analyse/optimize either a heliostat field and/or the entire solar thermal plant. Many of these codes are available as freeware, and allow the user greater/lesser freedom of choice in the variables to be optimized. Although some allow user specified field lay-outs, it would appear that their optimization capabilities are currently restricted to radial staggered or cornfield lay-outs.

2. Model description

2.1. Optical field efficiency

Heliostats close to the tower as a rule have a higher efficiency than those further away from the tower. This has led Noone et al [13] to sacrifice a little on blocking and shading efficiency in return for a higher density layout close to the tower. The overall result is a smaller plant footprint and a more efficient heliostat field. A biomimetic layout, similar to the petals on a sunflower, yields a continuous density function across the entire field. More significantly, it is amenable to mathematical optimization.

The position vector of heliostat k in polar coordinates for a phyllotaxic lay-out as suggested by Noone et al is given by

$$r_k = ak^b$$

and

$$\varphi_k = \frac{4\pi k}{3+\sqrt{5}}$$

Here, it is assumed that the land is perfectly flat, and that the Cartesian vector pointing from the centre of the heliostat to the centre of the receiver is given by

$$\vec{T}_k = \{-r_k \cos\varphi_k\,;\ -r_k \sin\varphi_k\,;\ H_t\}$$

with H_t the optical height of the tower. The cosine efficiency of the heliostat is given by

$$\eta_{c,k} = \cos\psi_k$$

With

$$\psi_k = 0.5\cos^{-1}\{\vec{t}_k \cdot \vec{s}_k\}$$

The unit vector $\vec{s}_k$ is pointing from the centre of the heliostat towards the sun, and $\vec{t}_k$ is the unit vector of $\vec{T}_k$. The sun vector is given by Duffie and Beckman [14]

$$\vec{s} = \cos\phi\sin\theta\,\vec{\imath} + \sin\phi\sin\theta\,\vec{\jmath} + \cos\theta\,\vec{k}$$

with θ and ϕ the sun zenith and azimuth angles respectively. The blocking and shading algorithm, based upon the projection of rectangular images of neighbouring heliostats onto each other is described in a sister publication by Hoffmann[15]. The method is expected to marginally overpredict blocking and shading effects. Noone's seeding algorithm does not allow a clear link between heliostat k and its immediate neighbours. Heliostats were checked for shading against all other heliostats in the field, whilst blocking calculations were restricted to those heliostats with lower indices, and consequently located closer to the tower.

A spillage loss was calculated by projecting a circular heliostat image onto a projection of the receiver in a plane normal to the incoming beam from heliostat k [16], allowing for a beam angle divergence of 9.3 mrad. No provision was made for canting of the mirror surfaces.

A constant extinction coefficient, adjusted to match the annual direct normal irradiation of 2 100 kWh/m^2/y as reported in the literature [17], was used to simulate attenuation losses in the troposphere. The model effectively assumes that every day is a sunny day, but with a relatively high turbidity factor to compensate for cloudy days. This approach bypasses the need for typical meteorological year data, and should have little effect on the integrated annual collected energy, but it is not recommended for design point calculations. It was assumed that the same extinction coefficient also holds at ground level. The atmospheric attenuation efficiency is given by

$$\eta_{at} = e^{-\kappa|\vec{r}_k|/11\,000}$$

Surface, astigmatism, tracking and sun shape errors were not taken into account. Mirror fouling and reflectivity were combined into a single constant efficiency η_r, whilst a constant availability η_{av} was assumed for the field. The total collected radiation is given by

$$Q = \sum_{n=1}^{365}\left[\sum_{t=sunrise}^{sunset}\left\{\sum_{k=1}^{N}\eta_{c,k}\eta_{b,k}\eta_{s,k}\eta_{s,k},\eta_{at,k}\eta_r\eta_{av}I(n,t)A_h\right\}\right]$$

A spot validation of the model was done against SolarPILOT v.2016.3.17 for solar noon on the spring equinox. Total

collected energy results are within 1.5 %, with this model yielding the more pessimistic result. SolarPILOT, using a convolution integral [18] for the sun shape, would assign lower flux values to the periphery of the image than the pill-box shaped assumed in this model, resulting lower spillage losses.

2.2. Field optimization

Parametric studies tend to explore the entire design space, and hence almost guarantee that the global minimum or maximum will be found. However, for problems with many design variables, a vast number of samples have to be taken from design space. If the sampling calculations are expensive to evaluate, a parametric study very soon becomes impractical. Mathematical optimization attempts to reduce the number of samplings (design iterations) significantly below that required for an equivalent parametric study.

Careful consideration should be given to the choice of objective function. In solar thermal power plants, key economic indicators (LCOE, maximum revenue, etc.) are often in conflict with key energy indications (heliostat field efficiency, total collected energy, etc.) necessitating the use of a multi-objective optimiser [8]. The cost of individual plant components and infrastructure, inflation and interest rates and feed-in tariffs are variable in time and across countries, rendering most economic evaluations temporal in nature and at the mercy of forecasts [19]. A decision was made to focus only on one key energy indicator, namely the total collected solar energy, despite LCOE being of more practical significance for plant owners.

The task is to maximize the annual collection of solar energy from the heliostat field

$$\max f(\vec{x}) = Q(a, b, H_t, H_r, D_r, L_h, W_h)$$

Subject to the non-interference constraint

$$g(\vec{x}) = \left|\vec{r}_i - \vec{r}_j\right|_{i\neq j} \geq \sqrt{H_h^2 + W_h^2} + \delta$$

with δ = 0.5 m.

The initial design was loosely based on a 50 MW_e equivalent of the Gemasolar (37.5625° N) solar thermal plant [20], with the seeding parameters taken from [13], and is given in table 1. The current model is based on local solar time, not local standard (clock) time, hence the longitude will have no influence on the results. The eccentricity of the earth's orbit around the sun is ignored.

Newton's method is a very efficient steepest gradient optimization algorithm that takes the curvature of the function to be optimized into account:

$$\vec{x}_{i+1} = \vec{x}_i - \frac{\nabla f(\vec{x}_i)}{H(\vec{x}_i)}$$

Sampling of the $N \times N$ Hessian matrix, with N the number of design variables, is computationally expensive as it involves the calculation of the second derivatives $\partial^2 f / \partial x_i \partial x_j$.

Variable	Value
Tower optical height, H_t	140 m
Receiver height, H_r	22.5 m
Receiver diameter, D_r	14.2 m
Heliostat width, W_h	12.65 m
Heliostat length, L_h	9.49 m
a	4.5
b	0.65

Table 1. Initial design variables

Snyman and Hay's [21] spherical quadratic optimization algorithm (SQA) was selected for its robustness and ease of implementation. Another benefit of their algorithm is that it determines its own step length. It appears to be stable and reliable, even for ill-posed problems. Snyman and Hay replaced the determinant of the Hessian matrix with the curvature of a simple spherical quadratic function

$$H(\vec{x}_i) \approx C_i = \frac{2\{f(\vec{x}_{i-1}) - f(\vec{x}_i) - \nabla^T f(\vec{x}_i)(\vec{x}_{i-1} - \vec{x}_i)\}}{[\![\vec{x}_{i-1} - \vec{x}_i]\!]^2}$$

The optimization problem is reduced to finding the minima of a sequential series of quadratic sub-problems instead. This greatly reduces the number of computationally expensive function evaluations per design iteration from the 28 required for the Hessian, to 7. Perturbations of 1 % of the current value of the design variables were arbitrarily chosen to calculate local gradients. Groenwold et al [22] insisted on convex spherical quadratic approxima-tions.

$$C_i = max[C_i^*, \alpha]$$

C_i^* is substituted for the Hessian, and α is a positive real number.

The optimization is terminated when

$$|f(\vec{x}_{i+1}) - f(\vec{x}_i)| \leq \varepsilon_1 \quad and \quad |\nabla^T j(\vec{x}_{i+1})| \leq \varepsilon_2; \ (\varepsilon_1, \varepsilon_2) \text{ small}$$

In common with all conjugate gradient based algorithms, SQA can't discern between local and global maxima, and should preferably be tested with different initial designs to ascertain that it would consistently find the same optimum.

3. Results and discussion

A total of 7 000 heliostats, including those that violate the non-interference constraint (de-activated), were evaluated, and the annual collected energy recorded, as shown in figure 1. The artificial cap on the number of heliostats is merely a mathematical convenience, as a larger number of heliostats will invariably increase the total collected energy. Linear upscaling, ignoring heliostat efficiency, of the 20 MW_e Gemasolar plant to a 50 MW_e equivalent sized plant resulted in an optical field with about 7 000 heliostats. The worst performing heliostats were systematically removed from the field, until the remaining heliostats are capable to deliver the required electrical output. Note the absence of a formal exclusion zone close to the tower: the non-interference constraint typically place the first allowable heliostat at a distance $H_t / r_{min} > 0.8$ from the tower. The collected energy reached a maximum of $Q^* = 1\,530$ GWh_t after 6 iterations, where after it started to decrease slightly.

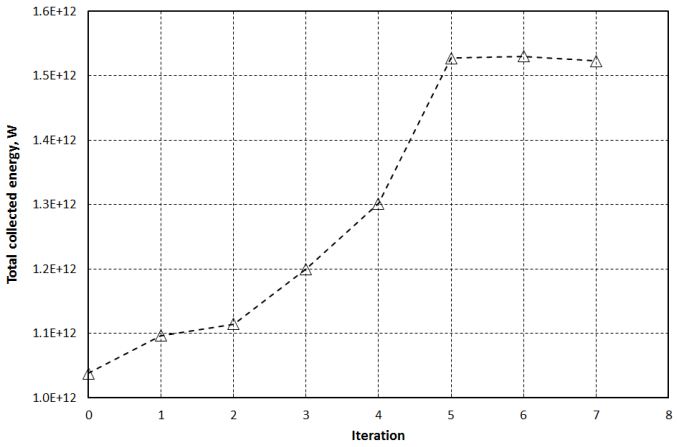

Figure 1. Total collected energy from entire field.

From figure 2, it is clear that heliostat length (26 %) and width (22 %), and receiver diameter (25 %) increased most significantly, whilst the tower optical height increased by only 9 %. The initial design specifications were for a tall, slender receiver. Receiver height and both the coefficient and exponent in the seeding function hardly moved from their initial values at all. The latter could be expected, as Noone et [13] already optimized their values. The results suggest that an aspect ratio close to 1 for both heliostats and receiver is desirable, something also observed by Ausburger [8]. However, the model assumes a single aiming point on the tower axis for all heliostats, without any constraint on the maximum receiver heat flux (not included in the calculations), and the lack of a proper aiming strategy might skew the receiver dimension results.

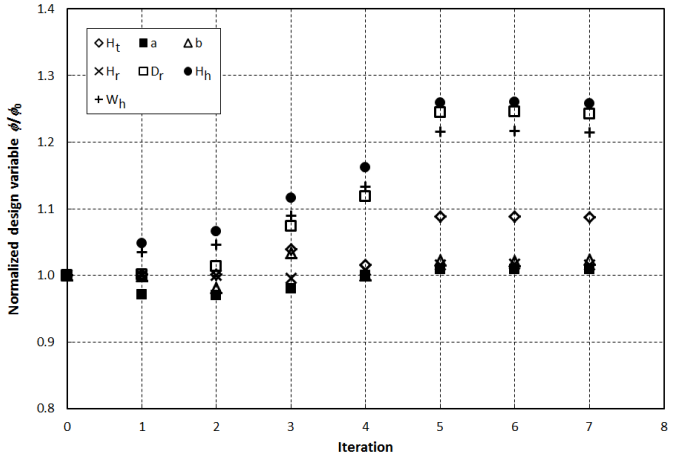

Figure 2. Migration of design variables towards optimum.

The final design variables are listed in table 2, with their percentage change from the original design in brackets.

Heliostats were ranked in descending order of collection efficiency, and the lowest ranked heliostats were removed from the field. The remaining heliostats were sufficient to deliver 50 MW_e continuously throughout the year for a plant with an average thermal efficiency of 40 %. Average here refers to the thermal efficiency at the average ambient temperature.

A number of heliostats closest to the tower are also eliminated as they violate the non-interference constraint. As a result, the exclusion zone close to the tower has a radius of 125.8 m, or 82.5 % of the tower optical height, that is deemed sufficient space for the power block, thermal energy storage and auxiliary plant. The final field lay-out, containing 4 284 heliostats, is depicted in figure 3.

Variable	Value (percentage change)
Tower optical height, H_t	152.4 m (8.9 %)
Receiver height, H_r	22.87 m (1.5 %)
Receiver diameter, D_r	17.69 m (24.5 %)
Heliostat width, W_h	15.39 m (21.6 %)
Heliostat length, L_h	11.96 m (26.0 %)
a	4.54 (0.9 %)
b	0.66 (2.1 %)

Table 2. Final design variables.

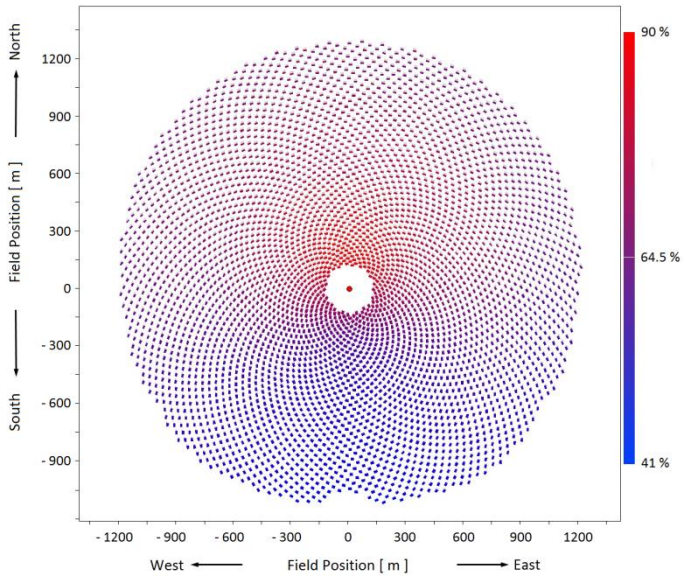

Figure 3. Heliostat field lay-out after 6 design iterations.

Iter	0	1	2	3	4	5	6	7
N_h	6917	6640	6668	6015	5377	4293	4284	4304
Q_{max} [GWh]	1038	1097	1115	1200	1301	1527	1530	1523

Table 3. Change in number of heliostats required to deliver 50 MWe throughout the year, and collected energy from all heliostats.

This study would suggest that the best optical performance is derived from 184 m^2 heliostats, based upon optical performance only. Ausburger [8] found that the lowest specific cost for heliostats falls within the range 200 $m^2 < A < 250$ m^2. Pidaparthi and Hoffmann [12] evaluated three discrete heliostat sizes, and reported that the lowest LCOE is achieved for 43 m^2 heliostats. Quite clearly, different objective functions drove these studies towards vastly different outcomes. The objectives seem to be conflicting, and Ausburger [8] reported that the unconstrained plant with the best LCOE also has the worst optical efficiency.

4. Conclusion

The optical performance of a 50 MW_e solar thermal power plant was evaluated for a location coincident with the Gemasolar solar thermal power plant in Southern Spain. Seven design variables, namely tower optical height, receiver height and diameter, heliostat length and width, and the two seeding variables for a biomimetic heliostat field layout were optimized, using a conjugate gradient method solving successive spherical quadratic sub-problems. Blocking and shading efficiency were determined from orthogonal mapping of heliostat images onto each other for the entire field, whilst spillage loss was calculated in a similar fashion by mapping a circular image of the heliostat onto the receiver. A spot validation of the model was done against SolarPILOT for spring equinox, and the model under predicted the collected energy by 1.5 %. Although the SolarPILOT code seems computationally more efficient, its current optimization capability is limited to internally generated, radially staggered and cornfield layouts, and does not allow for the optimization of user defined heliostat field layouts.

The optimal solution gravitated towards large (184 m^2), almost square heliostats and a large receiver with aspect ratio striving towards unity. At the optimum design, the annual average field collection efficiency was 64.0 % compared to the initial field efficiency of 57.7 %.

It is clear from the literature that different objective functions (cost per unit surface area, LCOE, collection efficiency, etc.) drive the optimal design in different directions, and that the use of a multi-objective optimizer, as suggested by Ausburger [8] would be prudent. It would appear that the choice of objective function is currently dictated by the role of researcher (plant owner/operator, heliostat developer/supplier, academic, etc.) in the solar thermal community. Literature suggests that there's currently a lack of consensus on an appropriate objective function amongst the solar thermal community.

References

[1] G.J. Kolb et al, (2007). Heliostat Cost Reduction Study, SANDIA National Laboratories Report SAND2007-3293.

[2] A. Pfahl, Survey of Heliostat Concepts for Cost Reduction, Journal of Solar Energy Engineering, 136 (2014) 14501–(1–9).

[3] J.B. Blackmon, Parametric Determination of Heliostat Minimum Cost per Unit Area, Solar Energy 97 (2013) 342–349.

[4] J.N. Larmuth et al, A Top-down Approach to Heliostat Cost Reduction, SolarPACES 2015, cape Town.

[5] F.W. Lipps and L.L. Vant-Hull, A Cellwise Method for the Optimization of Large Central Receiver Systems, Solar Energy 20 (1978) 505-516.

[6] M. Sánchez and M. Romero, Methodology for Generation of Heliostat Field Layout in Central Receiver Systems Based on Yearly Normalized Energy Surfaces, Solar Energy 80 (2006) 861 - 874.

[7] X. Wei et al, A New Method for the Design of the Heliostat Field Layout for Solar Tower Power Plant, Renewable Energy 35 (2010) 1970–1975.

[8] G. Ausburger, (2013). Thermo-Economic Optimisation of Large Solar Tower Power Plants, PhD Thesis, Swiss Federal Institute of Technology, Lausanne.

[9] S.M. Besarati and D.Y. Goswami, A Computationally Efficient Method for the Design of the Heliostat Field for Solar Power Tower Plant, Renewable Energy 69 (2014) 226 - 232.

[10] E. Carrizosa et al, (2014). An Optimization Approach to the Design of Multi-Size Heliostat Fields, Institute of Mathematics Report, University of Seville, Available from www.optimization-online.org/DB_FILE/2014/05/4372.pdf

[11] S.L. Lutchman et al, On Using a Gradient-based Method for Heliostat Field Layout Optimization, Energy Procedia 49 (2014), 1429 – 1438.

[12] A.S. Pidaparthi and J.E. Hoffmann, Effect of Heliostat Size on the Levelized Cost of Electricity for Power Towers, SolarPACES 2016, Abu Dabi.

[13] C.J. Noone, M. et al, Heliostat Field Optimization: A New Computationally Efficient Model and Biomimetic Layout, Solar Energy 86 (2012) 792–803.

[14] J.A. Duffie and W.A. Beckman, (2006). Solar Engineering of Thermal Processes, 3rd Edition, John Wiley & Sons, Hoboken, New Jersey.

[15] J.E. Hoffmann, Lumped Method for Calculating the Optical Efficiency of Radially Staggered Heliostat Fields, SASEC 2016, Stellenbosch.

[16] S. Lutchman, (2014). Heliostat Field Layout Optimization for a Central Receiver, MEng Thesis, Stellenbosch University.

[17] R. Guedez et al, Optimization of Thermal Energy Storage Integration Strategies for Peak Power Production by Concentrating Solar Power Plants, Energy Procedia 49 (2014) 1642 – 1651.

[18] F.W. Lipps, Four Different Views of the Heliostat Flux Density Integral, Solar Energy, 18 (1976), 555 - 560.

[19] G.S. Turchi and G.A. Heath, (2013). Molten Salt Power Tower Cost Model for the System Advisor Model (SAM), NREL Report NREL/TP-5500-57625, Golden, Colorado.

[20] O. Casas, (2014). Torresol Energy Press Dossier 2014, SENER Corporate Communication Report.

[21] J.A. Snyman and A.M. Hay, The Spherical Quadratic Steepest Descent (SQD) Method for Unconstrained Minimization with no Explicit Line Searches, Computers and Mathematics with Applications, 42 (2001) 169 – 178.

[22] A.A. Groenwold et al, Approximated Approximations for SAO, Structural and Multidisciplinary Optimization, 41 (2010), 39 – 56.